RSC Advances

PAPER

View Article Online
View Journal | View Issue

Cite this: *RSC Adv.*, 2023, **13**, 35209

Caffeic acid, a natural extract, as an activatable molecular probe for viscosity detection in a liquid system†

Lingfeng Xu, *[abc] Min Zhong,[a] Ziyin Tian,[a] Huilei Zeng[d] and Yanrong Huang*[e]

Received 10th August 2023
Accepted 13th November 2023

DOI: 10.1039/d3ra05423c

rsc.li/rsc-advances

Liquids, functioning as nutrients and energy systems, regulate various functions during storage programs. Microenvironmental viscosity is one of the most important physical parameters associated with the extent of deterioration, and it is crucial to monitor the mutation of viscosity at a molecular level. Herein, we utilized caffeic acid (**CaC**), a natural product extracted from thistles, as a molecular probe for viscosity sensing. **CaC** contains phenol hydroxyl (electron-donor) and carboxyl (electron-acceptor) groups, with both moieties connected by conjugated single and double bonds, forming a typical twisted intramolecular charge transfer system. The fluorescent probe **CaC**, obtained from a natural product without any chemical processing, exhibits high sensitivity ($x = 0.43$) toward viscosity, with an obvious visualized turn-on signal. Moreover, it displays good photostability, selectivity, and wide universality in commercial liquids. Utilizing **CaC**, we have successfully visualized viscosity enhancement during the spoilage process, with a positive correlation between the degree of liquid spoilage and microenvironmental viscosity. Thus, this study will provide a convenient and efficient molecular probe for food safety inspection across the boundaries of traditional biological applications.

Introduction

Viscosity, a vital physical parameter for liquids, is closely related to the dynamic changes in the microenvironment during the spoilage process, including transduction, metabolism, and apoptosis.[1,2] Liquids comprise additives such as various ions, amino acids, and vitamins and play a key role in the maintenance of nutrients and energy supplements; however, they also afford the growth of bacteria, causing deterioration of liquid food.[3] As a stress response and homeostasis mechanism, a change in the microenvironment may cause the movement of substances in a liquid food,[4,5] and the viscosity of fresh liquids (fruit juice, broth, or fresh liquids rich in nutrients) may be enhanced to a certain extent during the development of deterioration.[6,7] Abnormal changes in microenvironmental viscosity may provide a physical indicator during the deterioration process of some kinds of liquids (especially in the first couple of days), which is essential for early perception using a molecular probe in a sensitive, green, and *in situ* pathway.

Several traditional analytical methods based on several kinds of viscometers have been established.[8–11] When utilizing viscometers, large volumes of liquid foods are required, and the microscopic-scale molecular level cannot be measured.[12,13] In contrast, fluorescent techniques have enabled to transform the chemical and physical information into an optical signal, allowing the visualization of changes that occur in a liquid. Commonly, conjugated multifunctional molecular probes play a key role in the optical method as they offer unique advantages of rotational characteristics, remarkable sensitivity, non-invasiveness, simple pretreatment, and *in situ* features.[14–16] Currently, numerous reported probes have been developed by connecting electron donors and acceptors to form a twisted intramolecular charge transfer (TICT) system. These probes have various applications, such as tracking mitochondrial viscosity,[17] investigating lysosomal viscosity,[18] and sensing changes in physiological viscosity[19–22] (as collected in Table S1, ESI†). These fluorophores are mainly constructed *via* chemical synthesis methods, where a large number of organic solvents are consumed during the synthesis process. At present, low-carbon environmental protection has become the most popular development trend, and luminescent probes obtained from natural sources have attracted research interest. So far, several kinds of plant extracts have various applications, such as in Chinese Medicine, biological agents, and oral liquids.[23,24] Food spoilage

[a]*Institute of Applied Chemistry, School of Chemistry and Chemical Engineering, Jinggangshan University, Ji'an, Jiangxi 343009, China*

[b]*State Key Laboratory of Luminescent Materials & Devices, College of Materials Science & Engineering, South China University of Technology, Guangzhou 510640, China. E-mail: rs7lfxu@outlook.com*

[c]*School of Chemistry and Chemical Engineering, Nanchang University, Nanchang, Jiangxi 330036, China*

[d]*Ji'an Central People's Hospital, Ji'an, Jiangxi 343099, China*

[e]*School of Modern Agriculture and Forestry Engineering, Ji'an Vocational and Technique College, Ji'an, Jiangxi 343009, China*

† Electronic supplementary information (ESI) available. See DOI: https://doi.org/10.1039/d3ra05423c

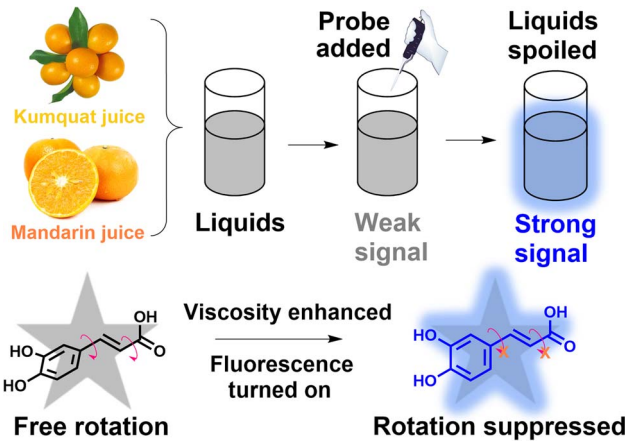

Scheme 1 Viscosity sensing and spoilage detection mechanism of CaC.

tracking has been studied based on the detection of substances such as toxic volatile amines,[25] allergens,[26] metal and ions[27,28] However, with the increasing concern about the evolution of sustainable long-term development, natural, green, and eco-friendly molecular probes urgently need to be exploited, and there is still large potential for their development in other fields (especially from the physical point of view).

In response to these considerations, herein, a natural molecular probe, caffeic acid (**CaC**), is extracted from thistles. It contains phenolic hydroxyl and carboxyl groups, which can act as an electron-donor (D) moiety and an electron-acceptor (A) moiety. The molecular probe can possibly be inhibited in a highly viscous microenvironmental liquid system, and the fluorescence signal can be released through the dissipative channel changing from nonradiative to radiative,[29,30] as displayed in Scheme 1. A D–π–A chemical structure is formed. The changes in viscous condition may afford the conversion of the excited state of **CaC** from the TICT state to the intramolecular charge transfer (ICT) state, which holds great potential for microenvironmental viscosity detection. Subsequently, with increasing viscosity, a maximum emission peak is exhibited at ~400 nm, and a "turn-on" mode is accompanied by a coefficient of $x = 0.43$. Additionally, **CaC** displays wide adaptability, good photostability, and excellent specificity toward viscosity change in commercial liquids. A suitable Stokes shift and high sensitivity coefficient can ensure its capability of real-time *in situ* tracking of the deterioration process. Compared with previous studies, **CaC** is extracted from a natural plant, avoiding complex design and synthesis processes and eliminating the need for any chemical modification procedure. The molecular probe **CaC** can not only track viscosity fluctuation during the spoilage process but also provide an opportunity for multifunctional molecular probes for interdisciplinary research.

Experimental sections

Materials and methods

The chemical reagents used in this study were obtained from Macklin Biotechnology (Shanghai) Co., Ltd, Anhui Energy Chemical Reagent Co., Ltd, and Shanghai Taitan Technology Co., Ltd. All the reagents and solvents were used without any further purification. Triple distilled water was used in the experiments. The reagents and instruments are described in the ESI.†

Extraction of natural product caffeic acid (molecular probe CaC)

Thistle was placed in an oven for 3 days. The dried plant was broken up and powdered. A sample typically containing 50 g of dried powder was placed in a Soxhlet extraction setup for 36 hours to extract caffeic acid. A green oil was obtained after storing the extracted oil for two or three days, and this oil was separated with the addition of KOH solution (10 M). The samples were filtered as required before the investigation of the chemical structure. Proton nuclear magnetic resonance (^{1}H NMR) (400 MHz, dimethylsulfoxide [DMSO]) δ 12.05 (s, 1H), 9.27 (d, J = 155.3 Hz, 2H), 7.43 (d, J = 15.9 Hz, 1H), 7.04 (s, 1H), 6.97 (d, J = 8.1 Hz, 1H), 6.77 (d, J = 8.1 Hz, 1H), 6.18 (d, J = 15.9 Hz, 1H). MS (ESI): m/z 179.03315 $[M–H]^+$, calcd for $C_9H_8O_4$ 180.04226.

Investigation of optical properties

An accurate weight of 1.8 mg of **CaC** was prepared in DMSO solution, and the stock concentration of **CaC** was controlled at 1 mM. Before the experiment, the stock solution was stored in the dark at low temperature. In the optical test, the concentration of **CaC** was diluted to 10 μM, and the **CaC** probe was added into systems with different viscosities which were made from mixtures of glycerol (0% to 99%) and distilled water, and the emission spectra were performed in these mixed systems. Absorption spectra were taken in glycerol and distilled water, respectively. A viscometer was also utilized to determine the viscous value. To estimate solvent adaptability, six representative liquid with varied polarities were selected: toluene, tetrahydrofuran, acetonitrile, *N*,*N*-dimethylformamide, DMSO, and water; the absorption and emission properties of **CaC** in the complex solvent environment were obtained. **CaC** was freshly prepared and added to every sample. To investigate the specificity of the complex environment in the liquid food, various analytes (including cations, anions, food additives, and glucose) were prepared as stock solutions, and **CaC** was added before the test. The detailed spectra and fluorescent intensities were recorded. Three representative temperatures were selected to test the effects of temperature on viscosity, 37 °C, 5 °C, and 25 °C, and each sample was contained in **CaC** solution with 1% DMSO. In a thickening experiment, three representative thickeners (from 1 g kg^{-1} to 5 g kg^{-1}) were dissolved in water to prepare viscous media: xanthan gum (XG), pectin (Pec), and sodium carboxymethyl cellulose (SCC). Before recording the spectra, the mixtures were stored at room temperature to eliminate bubbles. All optical properties were combined with the natural **CaC** and then transferred to a quartz cell, and an excitation wavelength of 320 nm was used.

Viscosity checking process

Two representative commercial liquids, kumquat and mandarin juices, were stored at 25 °C and 5 °C, respectively. The

storage process was recorded with digital images and fluorescence spectra. Then, the relationship between the fluorescence signal intensity and viscosity enhancement was established: $(\eta_n - \eta_0)/\eta_0 \sim (F_n - F_0)/F_0$, where F_n and F_0 represent the fluorescence intensity at day n and day 0, respectively, and η_n and η_0 represent the viscosity value at day n and day 0, respectively.

Theoretical calculation of the molecular probe

Theoretical calculations were operated using the Gaussian 09 program with the B3LYP/6-31G(d) level of theory, and the chemical structure of the natural molecular probe **CaC** was optimized at 0° and 90°, respectively. The energy gap and oscillator strength f_{em} were calculated.

Results and discussion

Molecular probe design and selected strategy

Recently, natural extracts have become a research topic, due to their degradable, sustainable, and reproducible features and rich resources. Fluorescence imaging technology can transform the chemical and physical signals into fluorescence intensities, allowing the visualization of microenvironmental fluctuations and viscosity changes. We found that *O*-diphenol can be displayed as an electron-donor (D) moiety and carboxyl as an acceptor (A) moiety. Coincidentally, both groups were hosted in the **CaC** natural molecule. A typical ICT structure was formed. We expected a free rotation phenomenon to occur between the *O*-diphenol and carboxyl groups, and the excited dye can be relaxed in a nonradiative pathway, which can lead to quenching of fluorescence. In contrast, the relaxation pathway can be affected when the microenvironmental viscosity increases; thus, the molecular rotation may be inhibited in the viscous condition. In this case, the excited state may be converted into a radiation transition pathway, which may increase the possibility of its state changing from TICT to ICT; thus, the fluorescence intensity may be increased. Consequently, the natural molecular probe exhibits an obvious spectral response toward viscosity, and the high-viscosity media can be discriminated from the lower-viscosity ones (in Scheme 1). The extracted **CaC** was adequately characterized by ^{1}H NMR and high-resolution mass spectrometry, which have been provided in Fig. S1–S3 (ESI).†

Optical properties toward viscosity

With this natural molecular probe in hand, corresponding optical properties of **CaC** in low-viscosity water and high-viscosity glycerol were tested to confirm whether it can respond efficiently to viscosity. Detailed spectra were shown in Fig. 1a and b, where it can be found that **CaC** displayed a slightly longer absorption wavelength and stronger fluorescence signal in glycerol, while a shorter absorption wavelength and weaker fluorescence signal in water, with a sharp emission peak at ~400 nm. This distinguished low-viscosity media from the higher-viscosity samples. The red-shifted phenomenon may be ascribed to the inhibited rotation and parallel stacking of molecules in the high-viscosity microenvironment. Particularly, six viscosity gradients (1.0–956.0 cP) were set up in a series of

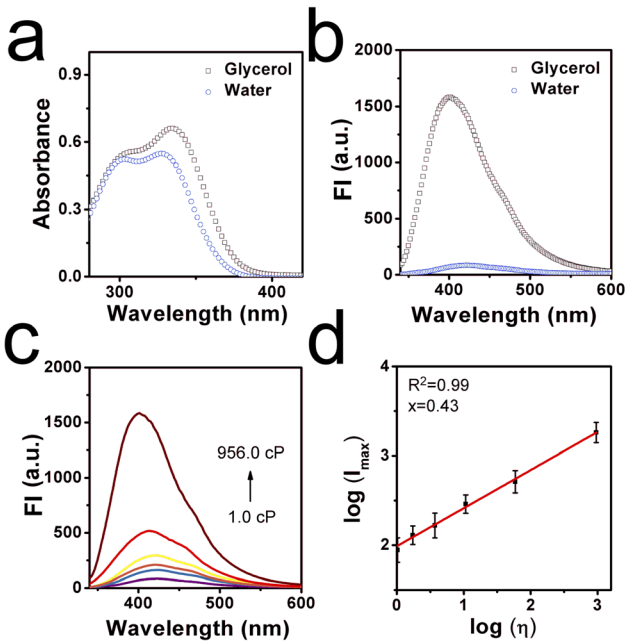

Fig. 1 (a) Absorption spectra of the molecular probe **CaC** in different solvents, such as water and glycerol. (b) Fluorescence spectra of the molecular probe **CaC** in different solvents, such as water and glycerol. (c) Fluorescence emissive spectra of molecular tool **CaC** in different solvent systems, with a water–glycerol mixture where the fraction of glycerol (f_g) ranges from 0% to 99%. (d) Linear relationship between log I_{433} and log η. $E_x/E_m = 0.8$; the probe concentration is 10 μM; the slit width: 10/10 nm.

water–glycerol mixture systems at a normal pH of 7.4. A varied viscosity microenvironment was established, and **CaC** was mixed in and fully dispersed (Fig. 1c and d). When the fraction of glycerol increased from 0% to 99%, the released fluorescence signal in the test system showed an obvious gradual turn-on phenomenon. The sensitivity coefficient x was calculated from $\log(I_{max})$ and $\log(\eta)$, which is the slope of the Förster–Hoffmann equation, where a higher value tends to show higher sensitivity toward changes in microenvironmental viscosity. Herein, a good linear relationship can be found between $\log(I_{max})$ and $\log(\eta)$, with a viscosity–sensitivity coefficient of $x = 0.43$. This result was fitted into the Förster–Hoffmann linear relationship (eqn (1) in the ESI†), and a turn-on mode was constructed. The final intensity was approximately 20 times the initial intensity. Subsequently, the Stokes shifts in water and glycerol were recorded from the absorption and emission spectra, as a larger Stokes shift may be helpful for filtering out spontaneous signals. In Fig. S4a and b (ESI),† the results showed 91.7 nm in low-viscosity water and 65.3 nm in high-viscosity glycerol. This result is similar to most previous probes designed through chemical synthesis trials (as displayed in Table S1, ESI†). Further, the effect of temperature on **CaC** in the process of viscosity detection was investigated, as viscosity is often affected by the temperature change processes. In Fig. S5 (ESI),† the fluorescence signal at 37 °C is weaker than that at 5 °C (lower-maintenance temperature), and a compromise temperature of 25 °C (ambient temperature) was used for the fluorescence signal. It can be concluded that viscosity may be enhanced with

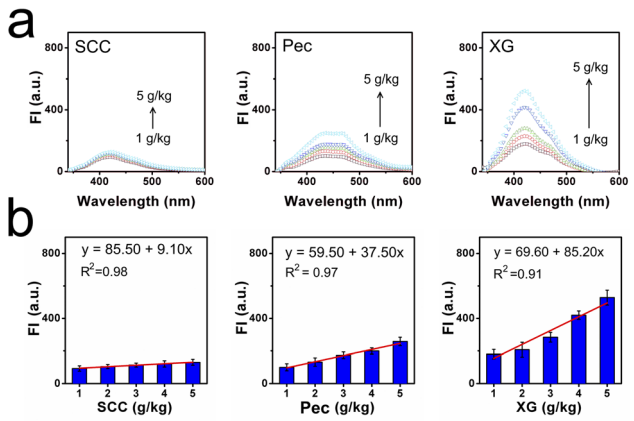

Fig. 2 (a) Emissive spectra of the molecular probe **CaC** in thickening solvents in the presence of various mass amounts of sodium carboxymethyl cellulose (SCC), pectin (Pec) and xanthan gum (XG). (b) Emission intensity of the molecular probe **CaC** in the corresponding thickening media, and fitting line with mass amounts of SCC, Pec, and XG.

a decrease in temperature, and a lower-maintenance temperature can to some extent enhance flavor and consistency, which may be closely related to viscosity. Next, the detection limit of **CaC** was investigated, and the regression curve equation was obtained under a lower-viscosity range, which was found to be 1.355 cP, as shown in Fig. S6 (ESI).† This is convenient for detecting viscosity in most common liquids.

Thickening efficiency is an important property of thickeners, and various viscosity microenvironments can be established with the addition of thickeners since thickeners can enhance the consistency, stability, and homogeneity of liquids. Thus, three representative thickeners were selected (in Fig. 2a and b): SCC, Pec, and XG. It was found that the fluorescence intensities were enhanced after the amount added increased from 1 g kg^{-1} to 5 g kg^{-1}, due to the thickening effects caused by these thickeners. Notably, the thickening efficiencies of these thickeners were quite different: the largest thickening slope of XG was 85.20, and the lowest thickening slope of SCC was 9.10. The thickening efficiency can be determined through the fluorescence method with **CaC**. Moreover, **CaC** was added to various commercial liquids to determine the viscosity through the fluorescence technique as well. The fluorescence signal intensities were observed, as shown in Fig. S7 (ESI).† Detailed data were collected in Table S2 (ESI),† and the calculated viscosity values obtained from the fluorescent method were consistent with the data obtained from a traditional viscometer, as shown in Table S3 (ESI).† The corresponding results further confirmed the great potential of **CaC** to image viscosity changes sensitively in liquids, especially in lower-viscosity media, and it can be utilized to visualize thickening effects.

Investigation of photostability, selectivity, and response mechanism

Photostability is another important property of **CaC**, and the fluorescence response of **CaC** in different kinds of liquid was investigated. As displayed in Fig. S8 (ESI),† the fluorescence intensity of **CaC** remains stable under continuous light irradiation for 60 min, when the signal is almost unchanged, indicating that the natural molecular probe **CaC** can maintain good photostability in most commercial liquids. Subsequently, **CaC** was added to solutions of various pH of different viscosities (Fig. S9, ESI).† The molecular probe **CaC** displayed a relatively stable signal in the different pH solutions, especially in the viscosity range above 1.8 cP, which shows that it possesses the ability to detect viscosity under wide physiological conditions. Moreover, the fluorescence signals are found to be stable at different common storage temperatures, as shown in Fig. S10 (ESI).† Slight changes in the fluorescence emission intensity can be captured, which may be attributed to minor changes in viscosity caused by the temperature. The effect of polarity in the liquid system is quite important, and it is necessary to investigate the stability of different kinds of solvents. Herein, we selected eight representative solvents, including glycerol and several kinds of common organic solvents. As shown in Fig. 3a and b, the absorption and emission spectra were investigated. It was found that only a slight bathochromic shift occurred in high-viscosity glycerol, and a significant signal was released in glycerol compared to other solvents; detailed fluorescence signals are visualized in Fig. S11 (ESI).† From these data, it can be seen that **CaC** is not influenced by polarity.

The liquid microenvironment is a complex system, containing various related additives, including ions, glucose, and vitamins. Therefore, a molecular probe needs to show good

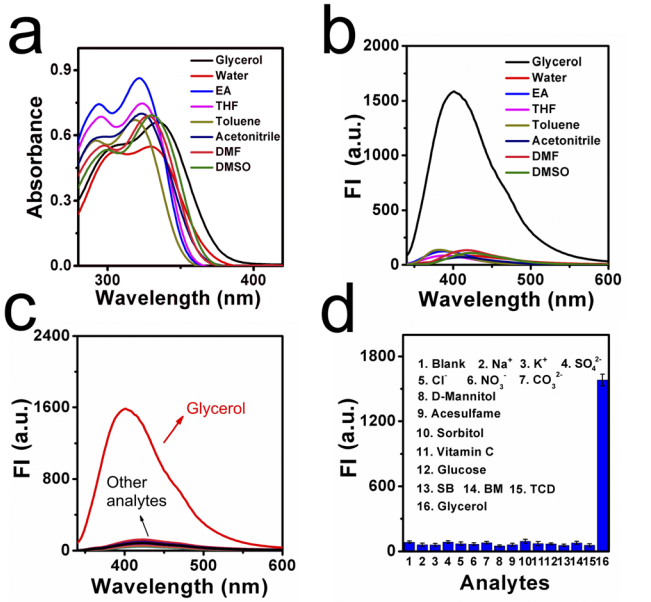

Fig. 3 (a) Absorption spectra of **CaC** (10 μM) in eight representative solvent. (b) Emission spectra of **CaC** (10 μM) in eight representative solvent. (c) Emission spectra of **CaC** (10 μM) in various solutions with potential analytes in liquid food. (d) Histogram of signal intensity of **CaC** with various analytes: (1) blank, (2) Na^+, (3) K^+, (4) SO_4^{2-}, (5) Cl^-, (6) NO_3^-, (7) CO_3^{2-}, (8) D-mannitol, (9) acesulfame, (10) sorbitol, (11) vitamin C, (12) glucose, (13) sodium benzoate (SB), (14) beet molasses (BM), (15) trisodium citrate dehydrate (TCD), and (16) glycerol. E_x/E_m = 0.8; the probe concentration is 10 μM; slit width: 10/10 nm.

selectivity to sense viscosity effectively. We studied the selectivity of **CaC** in various solutions with many kinds of representative species, including several kinds of cations, anions, and food additives. As shown in Fig. 3c and d, none of these analytes can cause significant changes in the fluorescence intensity of **CaC**, whereas an obvious turn-on signal can be found in glycerol. This indicates that **CaC** cannot be affected by various food additives and can maintain the released signal intensity toward viscosity in a complex liquid food system. Next, the solvatochromism of **CaC** was also measured. As shown in Fig. S12 (ESI),† a slight bathochromic shift occurred not only in the absorption spectra but also in the emission spectra, which may be ascribed to an ICT effect between the terminal donor and acceptor.

Based on the spectra data, the response mechanism of **CaC** toward viscosity sensing can be proposed. In low-viscous liquid foods, the free mechanical movement of molecules could be observed, and the nonradiative transition pathway of excited energy of the ICT was restored. Thus, the fluorescence intensity was weak. In contrast, intramolecular rotation was hindered; thus, the nonradiative pathway was reduced, and the fluorescence was enhanced. Then, a density functional theoretical calculation based on the Gaussian 09 package was utilized. The optimized structures of **CaC** at 0° and 90° are provided in Fig. S13 (ESI).† The electron density on the highest occupied molecular orbital is located in the *O*-diphenol group and the lowest unoccupied molecular orbital is positioned at the carboxyl unit. A pull–push electron system has been established, which may afford the ICT process. The energy gaps between *O*-diphenol (donor) and carboxyl (acceptor) can be calculated as 4.1953 eV at a dihedral angle of 0° and 4.6198 eV at an optimized 90°. The f_{em} (oscillator strength) was also calculated at 0° and 90° and was found to be 0.2597 and 0.0024, respectively. These theoretical calculations are consistent with the experimental results, which demonstrated that intramolecular rotation existed.

Deterioration process detection

CaC was further applied to detect the deterioration process due to its good optical properties and viscosity responsibility. Samples including kumquat and mandarin juices were divided into two groups. The first group was stored at ambient temperature, and the other group was used as control samples at a lower-maintenance temperature. Both groups were tested for 8 days, and the entire spoilage process was recorded using a digital camera and a fluorescence spectrometer. As displayed in Fig. 4a, when the kumquat and mandarin juices were stored at 25 °C (ambient temperature), both liquids gradually became turbid and opaque over time. In particular, within the next couple of days (after day 5), a serious floating phenomenon could be observed. With the help of **CaC**, the released signals of kumquat and mandarin juices became stronger (in Fig. 4c) and

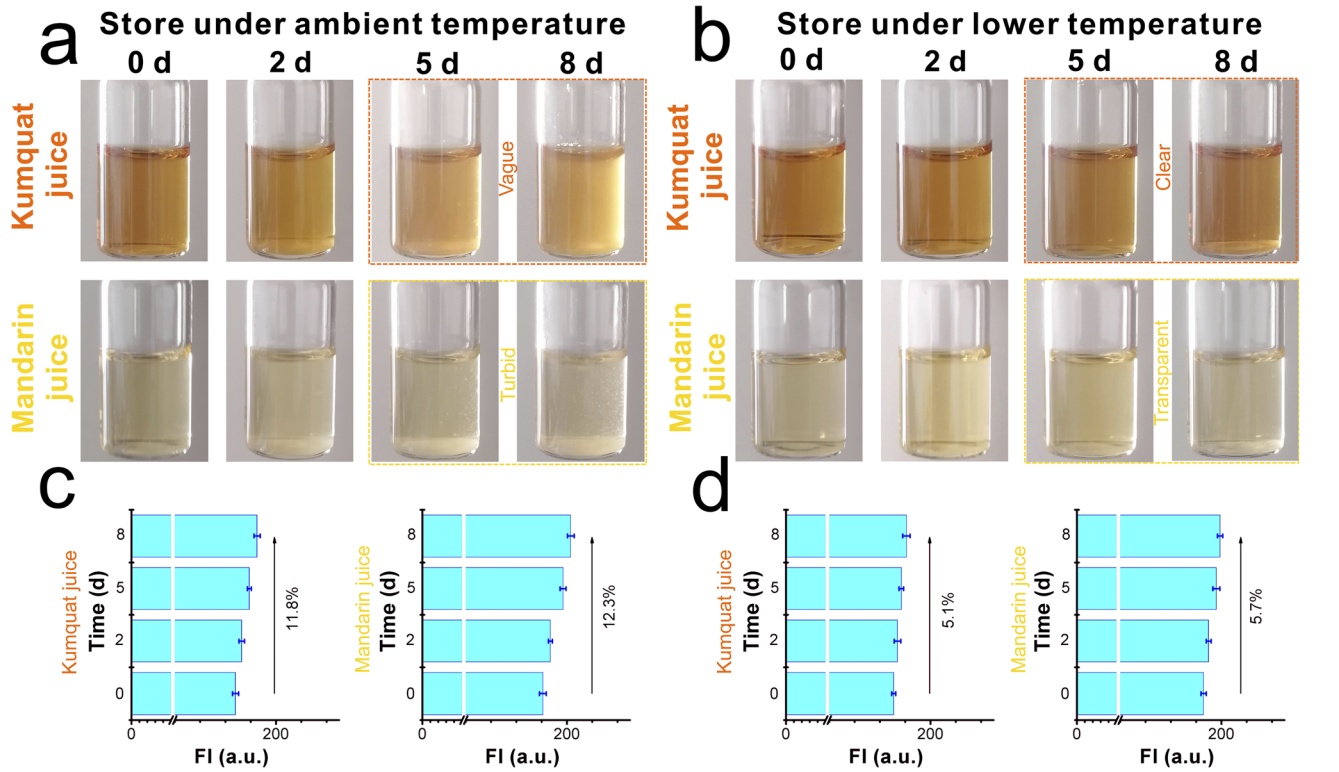

Fig. 4 Digital images of kumquat and mandarin juices stored at (a) ambient temperature and (b) fresh-maintenance temperature for varying times (from day 0 to day 8). The fluorescence spectra and enhancement of kumquat and mandarin juices during storage time (from day 0 to day 8) at (c) ambient temperature and (d) fresh-maintenance temperature. The concentration of **CaC** = 10 μM; λ_{ex} = 320 nm.

were found to be enhanced by 11.8% and 12.3%, respectively, at day 8. In contrast, when the control samples were stored at 5 °C (lower-maintenance temperature), the floating phenomenon had improved during the storage process, clear and transparent phenomena could be found, and there were only small floating objects (in Fig. 4b). From the fluorescence intensity perspective (in Fig. 4d), the signal enhancement was inconsistent with the apparent phenomenon: 5.1% in kumquat and 5.7% in mandarin. This shows that **CaC** can distinguish a normal liquid from a spoiled liquid, and abnormality in the microenvironmental viscosity during the spoilage process can be tracked using the spectrometer. Commonly, the pH values will shift to the lower direction as the sample is stored for a longer duration. Then, the natural probe **CaC** was added to the same pH ranges of samples and stored along with them for 8 days. The fluorescence intensities are recorded in Fig. S14 (ESI).† The FI changes were negligible during the storage timelines, indicating that the released fluorescence signal remained unaffected by immersion under acidic conditions.

From the quantitative perspective, viscosity values were also obtained using the viscometer. In Fig. 5a and b, on the one hand, the viscosity values of kumquat and mandarin juices stored at 25 °C were found to be enhanced by 25.6% and 28.2%, respectively. On the other hand, the viscosity values of these test samples at 5 °C were only enhanced by 10.5% and 12.1%, respectively. Both results obtained from the spectrometer and viscometer may yield a joint explanation: lower-maintenance temperature can extend the shelf life and delay the increase in viscosity.

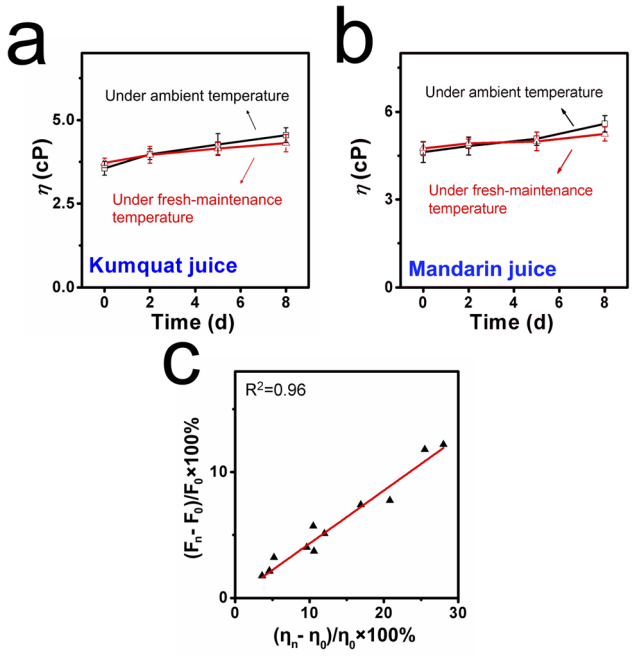

Fig. 5 (a) Viscosity values of kumquat juice when stored at different temperatures. (b) Viscosity values of mandarin juice when stored at different temperatures. (c) The fitted line between percentage increment in fluorescence and degree of viscosity enhancement.

To combine the fluorescence intensity and viscosity values, we established a fitting line between the enhancements in fluorescence intensity $(F_n - F_0)/F_0 \times 100\%$ and the changes in viscosity $(\eta_n - \eta_0)/\eta_0 \times 100\%$ (in Fig. 5c). Based on the corresponding results obtained from fluorescence technique and the traditional method, we can conclude that **CaC** has great potential for visualizing changes in microenvironmental viscosity, and, in particular, spoiled liquid foods can be distinguished from fresh ones.

Conclusions

To address the difficulty of identification of microenvironmental viscosity during the spoilage process of liquids and to avoid the consumption of a large amount of organic solvents during the preparation process, **CaC**, a kind of molecular probe, has been extracted from natural thistle plants. With rotatable single and double conjugated bonds in the chemical structure acting as the sensing point, a typical turn-on signal can be observed with an enhancement (20-fold) in microenvironmental viscosity. The sensitivity ($x = 0.43$), photostability, universality, and selectivity have been investigated. Based on the optical properties, this natural molecular probe has been applied in various commercial liquids, and different fluorescence intensities have been quantitatively determined. Importantly, there is an effective application of **CaC** for determination of microenvironmental viscosity during the liquid spoilage process. The recorded results from the spectrometer are consistent with those from a viscometer, which confirmed the viscosity-tracking capability of **CaC**. In addition, a linear relationship can be established between the fluorescence signal intensities and viscosity values from both methods. We believe that the natural molecular probe is crucial for building a powerful and promising molecular probe for broad application in interdisciplinary research. This probe is expected to practice the current trend of low-carbon sustainable development.

Author contributions

Lingfeng Xu: conceptualization, writing – original draft, methodology, funding acquisition. Min Zhong & Ziyin Tian: formal analysis, investigation. Huilei Zeng: validation, visualization, software. Yanrong Huang: resources, writing – review & editing.

Conflicts of interest

There are no conflicts to declare.

Acknowledgements

This study was supported by the Natural Science Foundation of Jiangxi Province (20232BAB204029), Science and Technology Program of Jiangxi Provincial Education Bureau (GJJ2209316), Ji'an City Science and Technology Plan Project Public Safety 1 ([2023]18, 20222-201751), Doctoral Research Foundation of Jinggangshan University (JZB2006), Ji'an Science and

Technology Plan Project (2023-043398), Research Fund of Jinggangshan University (JZ2301), Innovation and Entrepreneurship Training Program for College Students of Jinggangshan University (JDX2023126), and Innovation and Entrepreneurship Training Program for College Students of Jiangxi Province (S202310419039).

References

1 X. Yang, X. Lu, J. Wang, Z. Zhang, X. Du, J. Zhang and J. Wang, *J. Agric. Food Chem.*, 2022, **70**, 3047–3055.
2 Z. Wang, Y. Zhang, Y. Liang, M. Li, Z. Meng, Y. Yang, X. Xu and S. Wang, *J. Agric. Food Chem.*, 2022, **70**, 669–679.
3 P. Arora, A. Sindhu, N. Dilbaghi and A. Chaudhury, *Biosens. Bioelectron.*, 2011, **28**, 1–12.
4 S. Wibowo, C. Buvé, M. Hendrickx, A. Van Loey and T. Grauwet, *Trends Food Sci. Technol.*, 2018, **73**, 76–86.
5 F. Kweku Amagloh, A. N. Mutukumira, L. Brough, J. L. Weber, A. Hardacre and J. Coad, *Food Nutr. Res.*, 2013, **57**, 18717.
6 M. Ma, Q.-J. Sun, M. Li and K.-X. Zhu, *Food Chem.*, 2020, **318**, 126495.
7 X. Chai, Z. Meng and Y. Liu, *Food Chem.*, 2020, **317**, 126382.
8 J. Nsor-Atindana, H. Douglas Goff, W. Liu, M. Chen and F. Zhong, *Carbohydr. Polym.*, 2018, **200**, 436–445.
9 E. Lee, B. Kim and S. Choi, *Sens. Actuators, A*, 2020, **313**, 112176.
10 N. Mäkelä, O. Brinck and T. Sontag-Strohm, *Food Hydrocolloids*, 2020, **100**, 105422.
11 F. Morreale, R. Garzón and C. M. Rosell, *Food Hydrocolloids*, 2018, **77**, 629–635.
12 X. Liu, W. Chi, Q. Qiao, S. V Kokate, E. P. Cabrera, Z. Xu, X. Liu and Y.-T. Chang, *ACS Probes*, 2020, **5**, 731–739.
13 S. Ludwanowski, A. Samanta, S. Loescher, C. Barner-Kowollik and A. Walther, *Adv. Sci.*, 2021, **8**, 2003740.
14 H. Xiao, P. Li and B. Tang, *Chem.–Eur. J.*, 2021, **27**, 6880–6898.
15 J.-T. Hou, K.-K. Yu, K. Sunwoo, W. Y. Kim, S. Koo, J. Wang, W. X. Ren, S. Wang, X.-Q. Yu and J. S. Kim, *Chem*, 2020, **6**, 832–866.
16 Y. Tang, Y. Ma, J. Yin and W. Lin, *Chem. Soc. Rev.*, 2019, **48**, 4036–4048.
17 S. Li, P. Wang, W. Feng, Y. Xiang, K. Dou and Z. Liu, *Chem. Commun.*, 2020, **56**, 1050–1053.
18 J. Cui, H. Nie, S. Zang, S. Su, M. Gao, J. Jing and X. Zhang, *Sens. Actuators, B*, 2021, **331**, 129432.
19 X. Zhang, H. Yan, F. Huo, J. Chao and C. Yin, *Sens. Actuators, B*, 2021, **344**, 130244.
20 Z. Zou, Q. Yan, S. Ai, P. Qi, H. Yang, Y. Zhang, Z. Qing, L. Zhang, F. Feng and R. Yang, *Anal. Chem.*, 2019, **91**, 8574–8581.
21 L. Hu, D. Shi, X. Li, J. Zhu, F. Mao, X. Li, C. Xia, B. Jiang, Y. Guo and J. Li, *Dyes Pigm.*, 2020, **177**, 108320.
22 H. Li, W. Shi, X. Li, Y. Hu, Y. Fang and H. Ma, *J. Am. Chem. Soc.*, 2019, **141**, 18301–18307.
23 A. A. Elkordy, R. R. Haj-Ahmad, A. S. Awaad and R. M. Zaki, *J. Drug Delivery Sci. Technol.*, 2021, **63**, 102459.
24 C. Yao, J. Zhang, J. Li, W. Wei, S. Wu and D. Guo, *Nat. Prod. Rep.*, 2021, **38**, 1618–1633.
25 J. Hou, J. Du, Y. Hou, P. Shi, Y. Liu, Y. Duan and T. Han, *Spectrochim. Acta, Part A*, 2018, **205**, 1–11.
26 Y. Sun, X. Liang, J. Fan and X. Yang, *J. Photochem. Photobiol., A*, 2013, **253**, 81–87.
27 N. Duan, S. Yang, H. Tian and B. Sun, *Food Chem.*, 2021, **358**, 129839.
28 Y. Nural, E. Karasu, E. Keleş, B. Aydıner, N. Seferoğlu, Ç. Efeoğlu, E. Şahin and Z. Seferoğlu, *Dyes Pigm.*, 2022, **198**, 110006.
29 H. Su, J. Wang, X. Yue, B. Wang and X. Song, *Spectrochim. Acta, Part A*, 2022, **274**, 121096.
30 X. Feng, Y. Chen, Y. Lei, Y. Zhou, W. Gao, M. Liu, X. Huang and H. Wu, *Chem. Commun.*, 2020, **56**, 13638–13641.